JOURNAL OF OPTOELECTRONICS AND ADVANCED MATERIALS Vol. 9, No. 7, July 2007, p. 2116 - 2120

Preparation and characterization of polyvinyl alcohol – colloidal silver nanocomposites

C. N. CASCAVAL*, M. CRISTEA, D. ROSU, C. CIOBANU, O. PADURARU, C. COTOFANA
Institute of Macromolecular Chemistry "Petru Poni", 41A, Grigore Ghica Vodă Alley, 700487 Iaşi, Romania

The polyvinyl alcohol (PVA)-colloidal silver (Ag) nanocomposites were prepared mixing the colloidal Ag with PVA water solution, in presence of poly(diethylene adipate lactate) diol (PDEAL), The effect of very low amounts of colloidal Ag (below 50 ppm) on the PVA matrix was investigated. The neat PVA sample and PVA-colloidal Ag nanocomposites were characterized using transmission electron microscopy (TEM), scanning electron microscopy (SEM), differential scanning calorimetry (DSC) and as physico-mechanical behaviour. Both TEM and SEM techniques showed that the colloidal Ag was present inside of the PVA matrix as spherical particles in the nanometer dimensions, and as clusters. Mechanical analysis via stress-strain testing, as well as the dynamic mechanical analysis (DMA) showed a substantial increase of the mechanical properties of the nanocomposite materials, against those determined for the PVA matrix.

(Received April 6, 2007; accepted June 27, 2007)

Keywords: Nanocomposite, Colloidal Ag, PVA matrix, Nanoparticles

1. Introduction

Recently, metal nanocomposites have received a great interest due to their potential utilizations in microelectronics [1], photocatalysis [2, 3], magnetic devices [4], chemisorption and powder metallurgies [5]. Simultaneously, the hybrid systems consisting of metal nanoparticles and organic polymers display attractive assets for the benefit of nonlinear optics [6], photoimaging and pattering [7], sensor fabrication [8] and catalysis [9].

It has been recognized since ancient times that silver (Ag) and its compounds are effective antimicrobial and antiviral agents. Several chemical forms of Ag exhibit antimicrobial activities: Ag^+ ions in the form of Ag nitrate solution [10], tarnished bulk Ag [11] or nanometer-sized Ag particles [12, 13]. Nano-sized Ag particles have drawn much attention for their unique electrical and optical properties, such as quantum size effect (QSE) and surface plasmon resonance (SPR).

Polymers are considered good host materials for nanoparticles. Polymer nanocomposites have many potential applications in the fields of optics, electronics, mechanics, photoconductivity and so on. The Ag particles embedded into polymeric matrices influence and modify the polymer physical characteristics in a large measure [14-16]. Among the optical polymers, polyvinyl alcohol (PVA) is a water-soluble polymer, biodegradable and biocompatible [17-19]. PVA was extensively studied as the host for different kinds of nanofillers [20-23]. The investigations suggest that the introduction of nano-sized particles into PVA results in an optically functional composite material. In the last time, important attention has been devoted to the PVA-Ag nanocomposites [14, 24-28]. The PVA-Ag nanocomposite material presents importance due to the fact that PVA affords resistance to the composite and Ag confers its antimicrobial properties. In this way the hybrid material exhibits an exciting combination of properties that came both from PVA and Ag nanoparticles.

In the medical science there is questions weather or not Ag is a harmless agent for the human body, as well as on the toxicity level. In the previous papers reported on the PVA-Ag nanocomposites [14, 22, 24] the Ag content in PVA matrix varied between 1 and 5 wt. %. It was pointed out that the lower Ag content leads to the better capacity of Ag to penetrate the cell wall. The possible dangerous effect of the large quantities of Ag in biomaterials was our reason to investigate the effect of very low content of Ag nanoparticles (less than 50 ppm) on PVA matrix. This low concentration of Ag nanoparticles in PVA matrix was used with the main goal to have preliminary data regarding the morphology, the thermal, as well as the physico-chemical properties of PVA-Ag nanocomposites, before testing them as potential applications in medicine.

2. Experimental

2.1. Materials

PVA, with molecular weight between 65000 and 87000, was obtained from LOBA Feinchemie AG (Austria Chemical Companies). Colloidal Ag was purchased from ARGENOL S. L. laboratory (Saragossa, Spain). Poly (diethylene adipate lactate) diol (PDEAL), with number-average molecular weight 1800, was synthesized in our laboratory starting from adipic acid, lactic acid and diethylene glycol, as reported previously [29]. A direct condensation was carried out at 180^0C, time 6 h, under reduced pressure.

2.2 Preparation of PVA-Ag nanocomposites

PVA was dissolved in bidistilled water by stirring at 80 ^{o}C, time 6 h. The PVA-Ag nanocomposites were prepared by mixing the colloidal Ag and PVA-water solutions in different proportions. PDEAL, as plasticizer, was added to each mixture in the same proportion (PVA/PDEAL 70 wt%/30 wt%). Composite films with different concentrations (ppm) of Ag nanoparticles (Table 1) were obtained after the solvent evaporation at 110^{0}C, time 3 h.

Table 1. Samples composition.

Sample	Composition	Colloidal Ag (ppm)
PVA	-	-
2	PVA + PDEAL	-
3	PVA + PDEAL + Ag	20
4	PVA + PDEAL + Ag	30
5	PVA + PDEAL + Ag	40

2.3. Characterization

For transmission electron microscopy (TEM) measurements, 0.1 wt% PVA-Ag bidistilled water-solutions were embedded on the electrolytic grates, which were preliminarily covered with collodion and carbon. Evaporation was slowly carried out at the room temperature. TEM measurements were performed using a Tesla BS 5138 transmission electron microscope at 80 kV.

The scanning electron microscopy (SEM) was carried out using PVA-colloidal Ag films, which were fixed on aluminum support, by means of an electroconductor paste. A gold layer was preliminarily applied on the surface of the films. The studied samples were examined with a TESLA BS 301 scanning electron microscope.

DSC measurements were run on a DSC Mettler apparatus, in dynamic conditions (heating rate 10^{o}C/min).

The initial modulus of elasticity was measured at the room temperature using a TIRA-TEST 2161 apparatus; at a crosshead speed of 20 nm/min.

The dynamic mechanical analysis (DMA) was conducted using a Perkin-Elmer Diamond apparatus, provided with a standard tension attachment at a frequency of 1 Hz. The apparatus was heated between -80 and 200^{0}C (2^{0}C/min), in a nitrogen atmosphere. The films (20x10x0.5) were longitudinally deformed by small sinusoidal stress and the resulting strain was measured. The value of the storage modulus E', the loss modulus E'' and tension loss tangent (tan δ = E''/E') were obtained as a function of temperature.

3. Results and discussion

The morphological aspect of the studied samples was observed using TEM micrographs. The colloidal Ag in TEM experiments appears both as spherical particles and as particles with various geometrical forms, within nanometer dimensions. These particles are individualized, or are presented as agglomerations. Fig.1 shows some typical TEM images of PVA, PVA in mixture with plasticizer (sample 2) and PVA doped with Ag (sample 3 and sample 4). PVA sample shows an unstructurated homogeneous film. Sample 2 formed a less homogeneous film. Sample 3 and sample 4 with Ag in their texture present zones with particles, which are characteristic to the colloidal Ag- containing materials. The presence of Ag in the studied samples is confirmed by diffraction images, which consist in lights specific to the materials with monocrystalline forms.

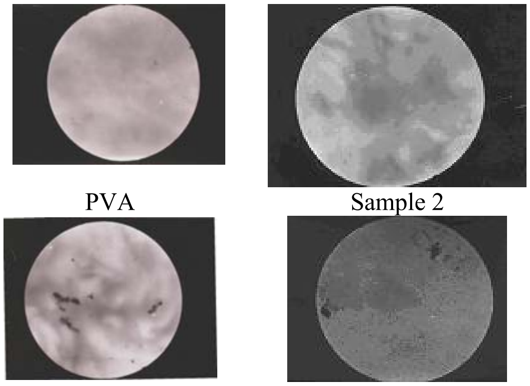
PVA Sample 2
Sample 3 Sample 4

Fig.1. The TEM images of PVA, PVA/ plasticize (sample 2) and PVA/plasticizer/colloidal Ag (sample 3 and sample 4).

Some morphological aspects regarding both the rugosity and the uniformity, as well as, the presence of Ag nanoparticles on the PVA surface were observed by means of SEM technique. SEM of the colloidal Ag is characterized by particles with various sizes and agglomerations. The PVA surface is smooth, without a topographical relief. Sample 2 points out the presence of some very pronounced crystalline zones (Fig.2). This means that PDEAL, added as plasticizer, has a strong influence on PVA matrix. It seems that the plasticizer enters into combination with PVA and modifies its morphological properties.

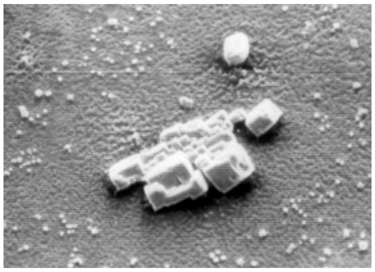

Fig. 2. The SEM image of the sample 2.

The samples with colloidal-Ag incorporated into PVA matrix show the presence of the Ag particles on the surface of the films, the surface having a rugose aspect and zones with round and/or ovoid forms. Fig.3 shows the SEM image of the sample 5, as an exemplification.

Fig. 3. The SEM image of the sample 5.

The thermal characterization of PVA-colloidal Ag nanocomposites was carried out by DSC technique. A summary of the DSC data is shown in Table 2.

Table 2. The glass transition temperature (Tg), the melting enthalpy and the crystallization heat of the studied samples.

Sample	T_g (^{0}C)	Melting enthalpy (J/g)	Crystallization heat (J/g)
PVA	63	42.7	17.9
2	60	33.6	37.3
3	60	32.8	32.7
4	60	33.1	35.2
5	60	34.5	39.4

As can be noted, a small decrease of Tg is remarked for the samples with Ag in their structures as against PVA. This is not in conformity with the results reported by Mihbele and co-workers [14]. The authors reported an increase of Tg with 20^{0}C using PVA samples doped with colloidal Ag (0.73 wt %). On the other hand, incorporation of magnetite particles into PVA matrix led to a decrease of Tg [24]. Conclusively, the Tg of PVA doped with inorganic particles depends on both the nature of the nanofiller and of the nanofiller content. Table 2 shows that the melting enthalpies are almost unchanged together with increase of Ag content in the PVA sample. This means that Ag nanoparticles act as the crystals thickening in the PVA matrix [14]. The increase of the crystallization heat for PVA-Ag samples, as against the pure PVA, means a modification of the PVA morphology, taking place an increase of the number of the crystalline zones in presence of the colloidal Ag.

Mechanical behaviour of the studied samples was also evaluated. Fig.4 shows the typical stress-strain curves for PVA, PVA with plasticizer and nanocomposites with different Ag loadings.

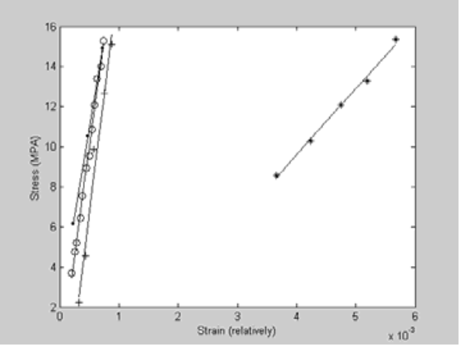

Fig. 4. Stress-strein curves for evaluation of the initial modulus of elasticity: PVA(--), sample 2(- o-), sample 3(-.-) and sample 5 (-+-).*

The curves in Fig.4 were used to evaluate the initial modulus of elasticity, defined as the initial elasticity work of the all inter- and intramolecular bonds in the polymer matrix, that are opposed to the stress in the elastic zone. Evaluation of the initial modulus of elasticity shows about six time increase of its value for the sample 2 (21823 MPa) as against the pure PVA (3312MPa). Depending on the Ag content, nanocomposite films show also a high increase of the initial modulus of elasticity (sample 3, 17491 MPa, and sample 5, 23475 MPa). The strong increase of the initial modulus of elasticity for the PVA-Ag nanocomposites indicates a significant reinforcement of the PVA matrix in presence of Ag nanoparticles. Our results regarding the mechanical properties are in a good agreement with the previous investigations of PVA-Ag nanocomposites [14], when the prepared nanocomposite films showed that the deformation behaviour is characteristic to a semi-crystalline type material.

DMA is a well-suited method used for the study of the miscibility of PVA/plasticizer/Ag composites and to emphasize the presence of the crystalline zones. Figure.5 shows the dynamic storage modulus E', the loss modulus E'', and tan δ versus temperature for pure PVA, PVA/PDEAL (sample 2) and PVA/PDEAL/Ag (sample 3 and sample 5).

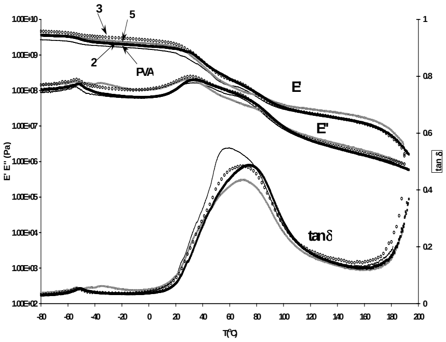

Fig. 5. The dependence on temperature of the storage modulus, the loss modulus and tan δ for PVA and modified PVA films (samples 2, 3, 5).

The drops in E’ curves and the peaks present both in E’’ and tan δ plots are due to the physical transitions in the polymer film. A weak and broad transition placed around -55 ^{0}C for the all analyzed films is a diagnostic for the presence of water [30]. It is known that, in the glass transition region, the storage modulus E’ displays an important decrease in a narrow temperature range. The plots in Fig. 5 evidence that the peak and the shoulder positions for the samples taken into consideration are difficult to establish using tan δ curves, due to their overlapping. In the case of PVA, a weak shoulder in tangent versus temperature curve corresponds to the β_a dispersion, due to the local relaxation mode of the PVA main chains. The E’ modulus starts to drop from 1.45×10^9 Pa at 30^{o}C, due to the glass transition process (α_a transition), till the first plateau beginning at 60^{o}C, with the elastic modulus 1.38×10^8 Pa. The dispersion observed above 60^{o}C in elastic modulus curve is due to the crystalline relaxation in PVA (β_c dispersion), distinguished as a small shoulder at 77^{o}C in the tan δ variation. The presence of the hydroxyl groups allows the chain to adopt a planar zig-zag conformation. All these transitions judged from the E’’ plots are summarized in Table 3. It is important to notice that the thermogram of PVA is a typical one for a water containing PVA. The Tg was significantly lowered by the plasticizing effect of water.

Table 3. Transitions in PVA and modified PVA films determined by DMA.

Sample	Underglass transition (^{o}C)	β_a (^{o}C)	T_g (^{o}C)	β_c (^{o}C)
PVA	-55	25	33	77
2	-51	27	35	80
3	-53.6	-	31	68
5	-53; -43; -33	-	30	84

A rubber like plateau in E’, above 100^{o}C, is observed at 3.10^{7}Pa and persists on temperatures up to 150^{o}C. As the temperature is further increased over 180^{o}C, the melting of the crystalline phase takes place, evidenced by a high upward shift in tan δ plot.

When PDEAL is blended with PVA there is no change in the onset of the Tg, relatively to that of pure PVA. Actually, the onset of T_g takes place about 20^{o}C for all blends. The loss modulus E’’ curve registers the glass transition shift slightly to higher temperature than PVA. In tan δ curve the fast edge of the distribution is moved to higher temperatures. The result indicates that the crystalline dispersion of PVA becomes more important in the sample 2. Moreover, the DMA studies confirmed the existence of a single T_g for the PVA/PDEAL mixture The miscibility is considered as being due to the interactions between the hydroxyl groups of PVA and carbonyl groups of PDEAL plasticizer. The introduction of Ag into the mixture induces a pronounced decrease in tan δ amplitude. This fact suggests that there are regions in PVA films where the mobility of PVA chains is reduced by the presence of Ag. Furthermore, it diminishes the Tg to 31^{o}C. It is noticed in E’ curve the increase of stiffness both of PVA and PVA/PDEA samples. The shoulder in E’’ plot at 68^{o}C confirms the presence of the crystalline zones, and the melting of the crystalline phase starts earlier, as revealed by the tan δ curve. The magnitude of tan δ peak decreases with increase of the Ag content. These results suggest that a phase-separated system can be produced, indicating a certain lack of homogeneity for the samples containing colloidal Ag.. The T_g is lower, but the crystalline zones appear at higher temperature (84^{o}C).

4. Conclusions

The PVA-colloidal Ag nanocomposites were prepared using PVA, as matrix, and colloidal Ag in very low amounts (bellow 50 ppm). The PVA-colloidal Ag mixtures contained and PDEAL with molecular weight 1800, as plasticizer The low concentration of Ag in PVA matrix was tested regarding both the morphology and the physico-mechanical properties of PVA-Ag nanocomposites.

The morphological aspect of the studied samples was observed both by TEM and SEM micrographs. The samples with colloidal Ag incorporated into PVA matrix showed the presence of Ag as spherical particles and as particles with various geometrical forms, within nanometer dimensions.

The thermal characterization of PVA-colloidal Ag nanocomposites was carried out by DSC technique. The increase of the crystallization heat of PVA-Ag samples, as against pure PVA, means a modification of the PVA morphology.

Mechanical analysis via stress-strain testing showed a substantial increase of the initial modulus of elasticity of the nanocomposite materials, compared with the values obtained for the pure PVA matrix. This means a significant reinforcement of the PVA matrix in presence of the colloidal Ag nanoparticles. DMA analyses showed a good miscibility between PVA and PDEAL plasticizer, the increase of stiffness, an increase of the crystalline zones for PVA mixed with PDEAL, and the decrease of the mobility of PVA chains, due to the presence of the colloidal Ag.

References

[1] G. Schmid, Chem. Rev. **92**, 1709 (1992).
[2] H. Hirai, Wakabayashi, M. Komiyama, Chem Lett. **1983**, 1047 (1983).
[3] K. Ghosh, S. N. Maiti, J. Appl. Polym. Sci. **60**, 323 (1996).
[4] J. M. Thomas, Pure Appl. Chem. **60**, 1517 (1988).
[5] J. A. A. J. Perenboom, P. Wyder, P. Meier, Phys. Rep. **78**, 173 (1981).

[6] M. Jose-Yacaman, R. Perez, P. Santiago, M. Benaissa, K. Gonsalves, G. Carlson, Appl. Phys. Lett. **69**, 913 (1996).
[7] A. S. Korchev, M. J. Bozack, B. J. Slaten, G. Mills, J. Am. Chem. Soc. **126**, 10 (2004).
[8] F. P. Zamborini, M. C. Leopold, J. F. Hicks, P. J. Kulesza, M. A. Malik, R. W. Murray, J. Am. Chem. Soc. **124**, 8958 (2002).
[9] V. M. Rudoy, B. G. Ershov, N. L. Sukhov, O. V. Dement′eva, V. Zaitseva, A. F. Seliverstov, M. E. Kartseva, V. A. Ogarev, Colloid J. **64**, 755 (2002).
[10] A. L. Rogach, G. P. Shevchenko, Z. M. Afanas’eva, V. V. Sviridov, J. Phys. Chem. B **101**, 8129 (1997).
[11] F.-R. F. Fan, A. J. Bard, J. Phys. Chem. B **106**, 279 (2002).
[12] E. B. Barmatov, D. A. Pebalk, M. V. Barmatova, Langmuir **20**, 10868 (2004).
[13] C.–N. Lok, C.–M. Ho, R. Chen, Q.–Y. He, W.–Y. Yu, H. Sun, P. K.–H. Tam, J.–F. Chiu, C.–M. Che, J. Proteome Res. **5**, 916 (2006).
[14] Z. H. Mbhele, M. G. Salemane, C. G. C. E. van Sittert, J. M. Nedeljkovic, V. Djokovic, A. S. Luytet, Chem. Mater. **15**, 5019 (2003).
[15] H. Behar-Levy, G. E. Shter, G. S. Grader, D. Avnir, Chem. Mater. **16**, 3197 (2004).
[16] T. Ung, L. M. Liz-Marzan, P. Mulvancy, J. Phys. Chem. B **105**, 3441 (2001).
[17] S. Kubo, J. F. Kadla, Biomacromolecules **4**, 561 (2003).
[18] K. Aoi, R. Nakamura, M. Okada, Macromol. Chem. Phys. **201**, 1059 (2000).
[19] M. G. Cascone, B. Sim, S. Downes, Biomaterials **16**, 569 (1995).
[20] M. C. Paiva, B. Zhou, K. A. S. Fernando, Y. Liu, P. E. Lopez, W. T. Pennington, J. M. Kennedy, Y. P. Sun, Composite Interfaces **12**, 757 (2005)
[21] N. Ogata, S. Kawakage, T. Ogihara, J. Appl. Polym. Sci. **66**, 573 (1997)
[22] K. E. Strawhecker, E. Manias, Chem. Mater. **12**, 2943 (2000)
[23] A. Bandyopadhyay, M. De Sarkar, A. K. Bhowmick, J. Polym. Sci. Part B: Polym. Phys. **43**, 2399 (2005).
[24] S. Porel, S. Singh, S. S. Harsha, D. N. Rao, T. P. Radhakrishnan, Chem. Mater. **17**, 9 (2005).
[25] W.-C. Lin, M.-C. Yang, Macromol. Rapid Commun. **26**, 1942 (2005).
[26] T. Vo-Dinh, D. L. Stokes, G. D. Griftin, M. Volkan, U. J. Kim, M. I. Simon, J. Raman Spectrosc. **30**, 785 (1999)
[27] J. Chih-Chao, J. Appl. Polym. Sci. **60**, 605 (1996).
[28] L. B. Luo, S. H. Yu, H. S. Qian, T. Zhou, J. Am. Chem. Sci. **127**, 2822 (2005)
[29] C. Ciobanu, G. Stoica, C. N. Cascaval, D. Rosu, L. Rosu, M. State, A. Emandi, I. Nemes, F. Petrescu, J. Appl. Polym. Sci., **103**, 659 (2007).
[30] J. Chih-Chao, J. Appl. Polym. Sci. **60**, 605 (1996).

---

[*] Corresponding author: cascaval@icmpp.ro